

Estimation of Land Surface Temperatures from Satellite Images for Al-Hammar Marshes in Iraq

Ashraf S. Abdulla¹, Bushra Q. Al-Abudi², Mohammed S. Mahdi³

^{1,2}Astronomy and Space Department, College of Science, Baghdad University, Baghdad, Iraq

³Computer Science Department, College of Science, Al-Nahrain University, Baghdad, Iraq

Abstract: Remote sensing instruments are key players to study and mapping land surface temperature (LST) at temporal and spatial scales. In this paper, Land surface temperatures for Al-Hammar Marshes in Iraq are estimated for years 1991, 2000, 2015, and 2017 using ENVI 5.1 software programming for the purpose of knowledge the extent of the change in surface temperature of the Marshesland by producing digital maps and classified chromatically to the temperature distribution and by taking advantage of the thermal band of the satellite Landsat sensors TM, ETM+ and OLI. By comparing four different time periods (1991, 2000, 2015 and 2017), we concluded that the surface temperature of Al-Hammar Marshes continued increase. The results indicated that the study area suffering from a clear increase in temperatures, included all classes of Marshesland, where the average temperature for the year 1991 approximately 41.506°C, while the average temperature value for the year 2000 increased about 44.69°C, an increase of 3.19 °C. for the year 1991. The average temperature for the year 2015 was approximately 47.31°C, an increase of 2.62°C for the year 2000, while The average temperature for the year 2017 was approximately 47.85°C and an increase of 6.35°C in comparison with the year 1991.

Keywords: Land Surface Temperatures, Landsat satellite images, thermal band, Al-Hammar Marshes

1. Introduction

Remote Sensing is the noncontact recording of information from the ultraviolet, visible, infrared and microwave regions of the electromagnetic spectrum by means of instruments such as cameras, scanners, lasers, linear arrays, and/or area arrays located on platforms such as aircraft or space craft and the analysis of acquired information by means of visual and digital image processing [1]. Image acquired by a scanner that records radiation within the thermal infra red band (3-5 μm and 8-14 μm) is used to measure the Land Surface Temperature (LST). Most temperature related studies have used polar orbiting satellite systems because of their high spatial and spectral resolution [2]. LST is an important factor in many areas of studies, such as global climate change, hydrological and agricultural processes, and urban land use/land cover. Calculating LST from remote sensed images is needed since it is an important factor controlling most physical, chemical, and biological processes of the Earth [3]. Land Surface Temperature (LST) can be defined as the temperature of the surface, which we observe if directly contact or touch it with or skin temperature of the surface of the earth or it is the temperature emitted by the surface [4]. Thermal infrared data in the remote sensing can help us obtain quantitative information of surface temperature. The Landsat TM, ETM+ and OLI sensors images can be used to study relation between surface temperature and land cover types using thermal quantitative indicators. S. Zareie et al. [5] used the temperature-emissivity separation (TES) algorithm for LST retrieving from the TIRS (Thermal Infrared Sensor) data of the Landsat Thematic Mapper (TM). The root mean square error (RMSE) and coefficient of determination (R²) were used for validation of retrieved LST values. Suresh et al., [6] applied single window algorithm methods to calculate the LST from TIRS. The heat energy radiated by the earth's surface determine factors such as different land use types, vegetation cover and soil in the study area reveals

the variation in surface temperature of different surface patterns. Surface temperature variation controls the surface heat and water exchange with the atmosphere resulting climatic change in the region. Though some climatic phenomenon play a minor role in temperature variation.

2. Study Area

The area under investigation is Al-Hammar Marsh. Iraqi Marshes is important as they have economic, social and biodiversity value. The marshes severed from many change from 1980 to this time because many dry in the end century. These drying operation have result in drastic change in the marshes environment which is still suffered until today. After 2003 the marshes were refilled but degradation in water quality and ecosystem still endures. Al-Hammar marshes is one of the three biggest marshes are located in the southern parts of Iraq, is situated to the south of the Euphrates river they are approximately bounded by the following coordinates (longitude 30° 45' - 30° 59' N, latitude 46° 25' - 47° 15' E") and has an area ranging from 2800 km^2 of contiguous permanent marsh to 4500 km^2 during flooding periods. In 2016 the UNESCO inscribed property is the fifth site from Iraq to be included in the World Heritage List, after Ashur, Hatra, Samarra Archeological city and Erbil Citadel. Figure (1) shows the original map of Iraq and location of study area within Iraq. In this work, we used four types of Landsat satellite images, because of its low cost, especially in relation to the area covered. Another advantage of Landsat images is the copyright, which permits a legal sharing of data among government department, academia and donor agency. Four types of satellite image were consulted during the work, Landsat-5 (TM) satellite image (5/6/1991 and 14/6/1991), Landsat-7 (ETM+) satellite image (6/6/2000 and 13/6/2000) and Landsat-8 (16/6/2015 and 23/6/2015) and (OLI) satellite image (5/6/2017 and 12/6/2017) with (Path/Row166/39) and (Path/Row167/39). These images were taken during the same season

(summer season), where not highly affected by atmosphere (scattering and absorption) and where clouds free. All three images are geometrically projected using Universal Transformed Mercator (UTM) coordinate system and World Geodetic System 1984 (WGS84) zone 38 and obtain from the USGS Earth Explorer database.

3. Methodology

In this section, land surface temperature of thermal band for Al-Hammar marshes were estimated using ENVI software programming of thermal bands, generate the temperature color map and analysis their spatial variations using Landsat 7 science data users handbook and Landsat 8 data users handbook procedures. These thermal bands are, thermal band 6(10.4 nm-12.5 nm) with 120 meter resolution for year 1991 (see figure 2); thermal band 6(10.4-12.5 nm) with 60 meter resolution for year 2000(see figure 3); thermal band 10(10.6nm-11.19nm) with 100 meter resolution for year 2015 and 2017 (see figures 4 and 5). Figure (6) illustrates the block diagram of estimation land surface temperature. Figures (7-10) show thermal band of satellite image after applying mosaic process for year 1991, 2000, 2015 and 2017, respectively. While figures (11-14) show thermal band of satellite image after applying clipping process for years 1991,2000,2015 and 2017,respectively.

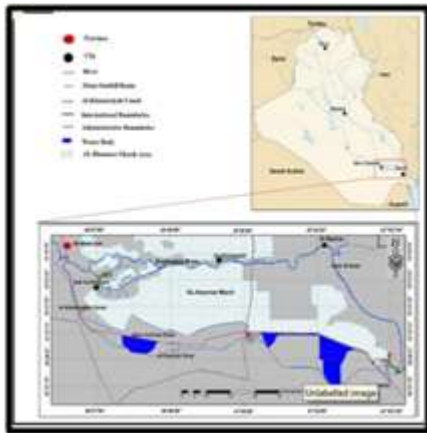
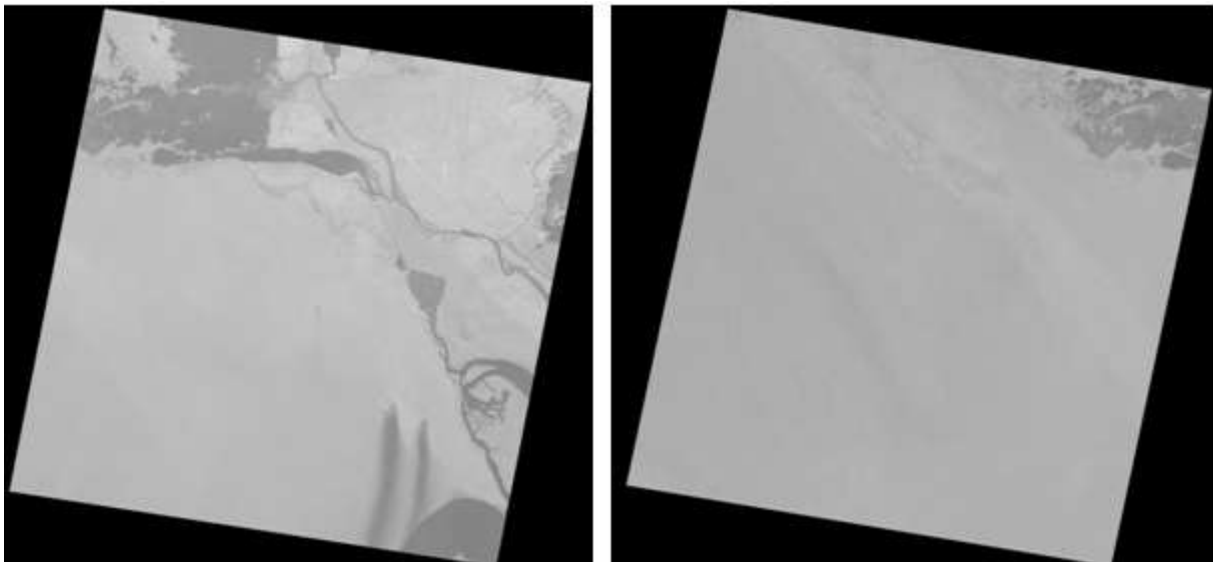
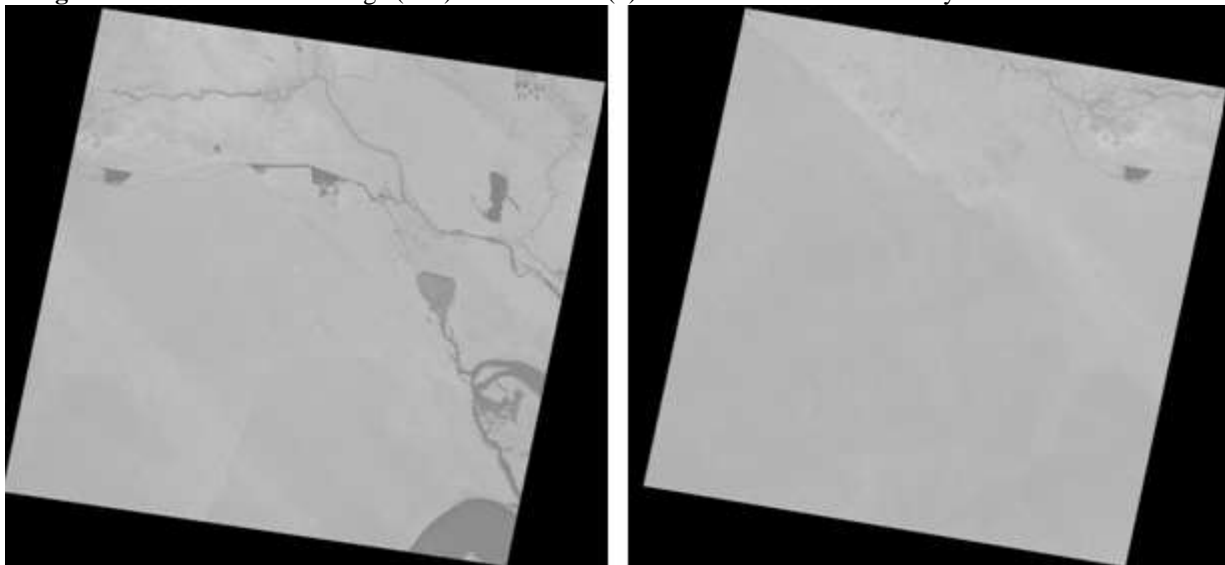


Figure1: Location of Study area within Iraq



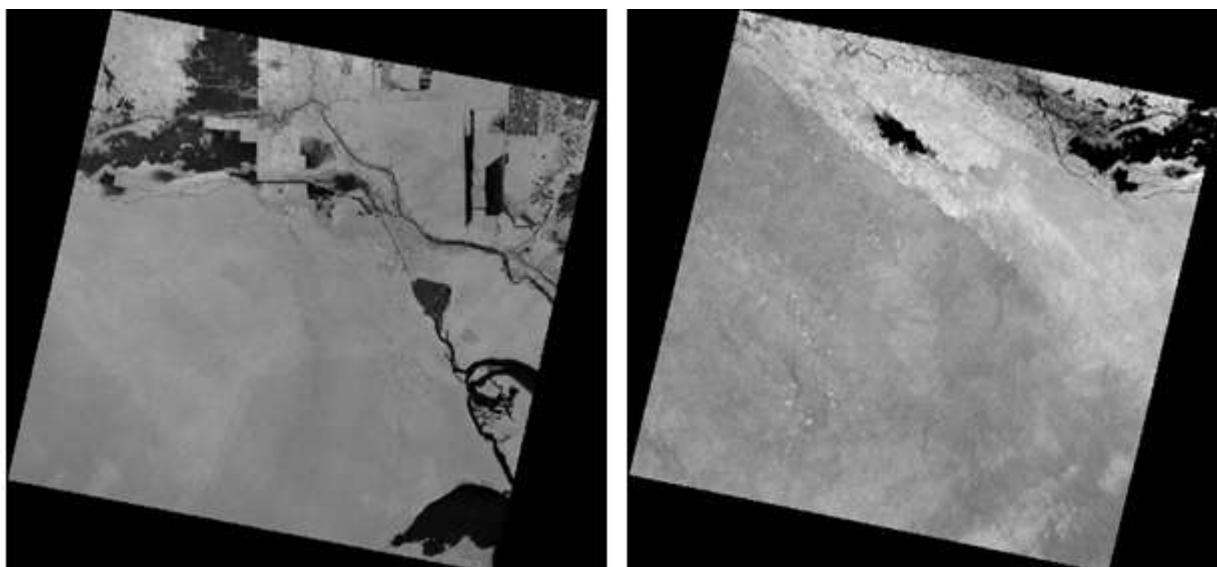
A) -Thermal band Row/Path 166/39 B) -Thermal band Row/Path 167/39

Figure 2: Landsat satellite image (TM) thermal band (6) of Al-Hammar Marshes for year 5/6 and 14/6/ 1991



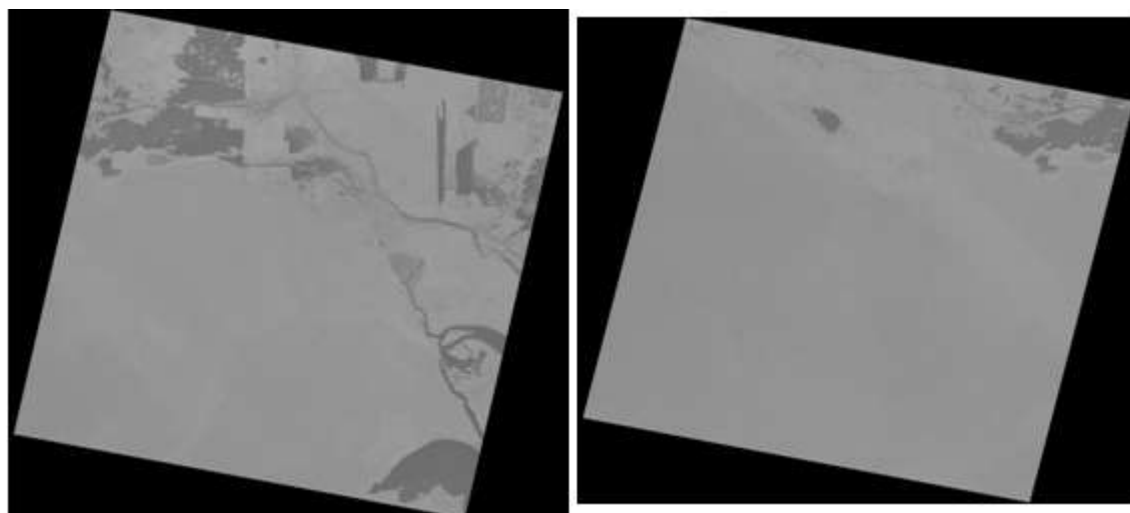
A) -Thermal band Row/Path 166/39 B) -Thermal band Row/Path 167/39

Figure 3: Landsat satellite image (ETM+) thermal band (6) of Al-Hammar Marshes for year 6/6 and 13/6/2000



A)-Thermal band Row/Path 166/39 B)-Thermal band Row/Path 167/39

Figure 4: Landsat satellite image (OLI) thermal band (10) of Al-Hammar Marshes for year 16/6 and 23/6/2015



A) Thermal band Row/Path 166/39 B) Thermal band Row/Path 167/39

Figure 5: Landsat satellite image (OLI) thermal band (10) of Al-Hammar Marshes for year 5/6 and 12/6/ 2017

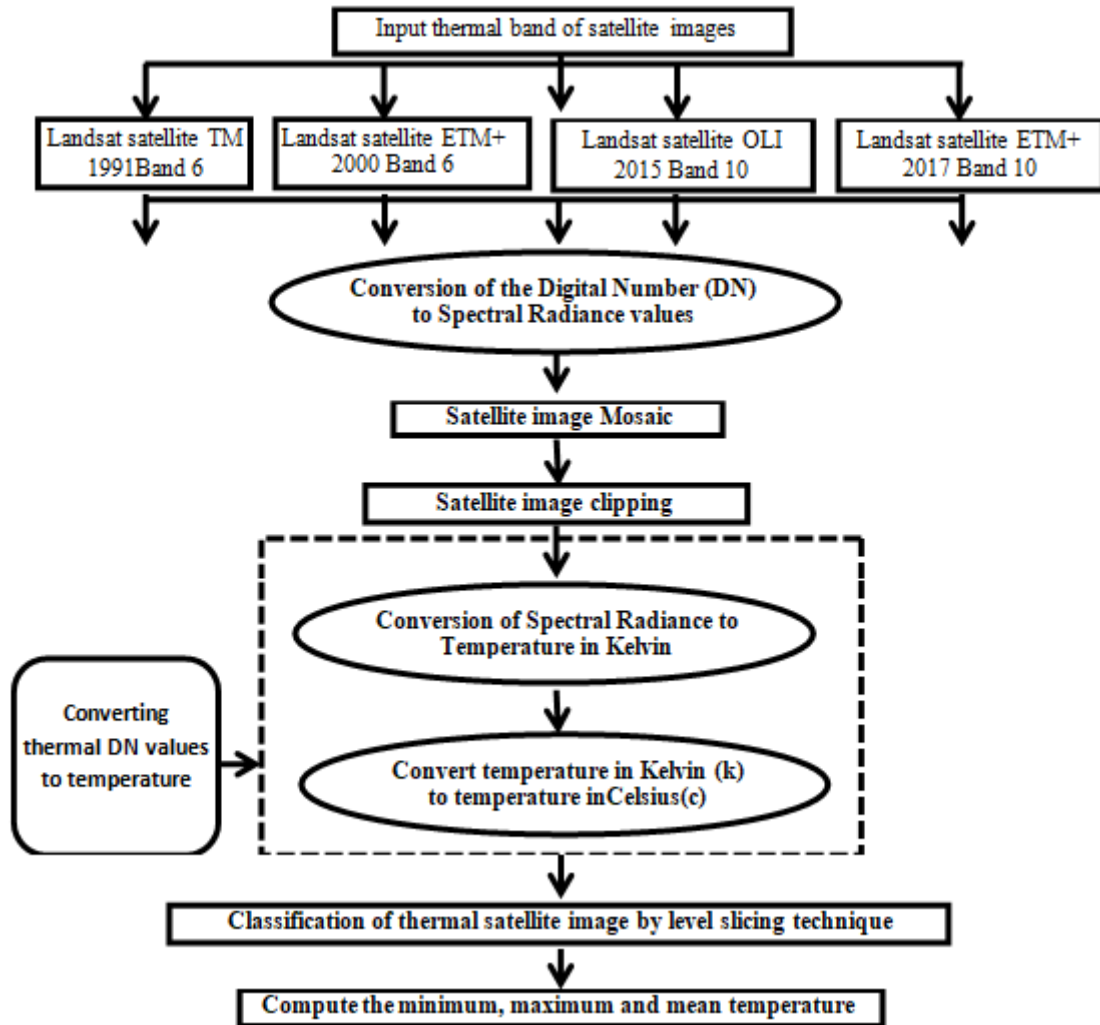


Figure 6: The block diagram of estimation land surface temperature for thermal bands of satellite image using EVNI programming

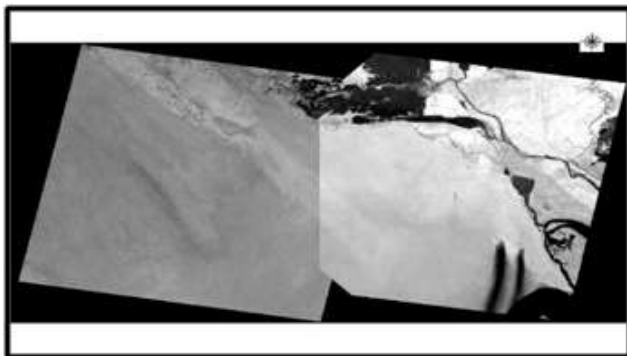


Figure7: Mosaic Landsat TM (5/6/1991 and 14/6/1991) band (6) for two satellite images Path/Row 166/39) and (Path/ Row 167/39)

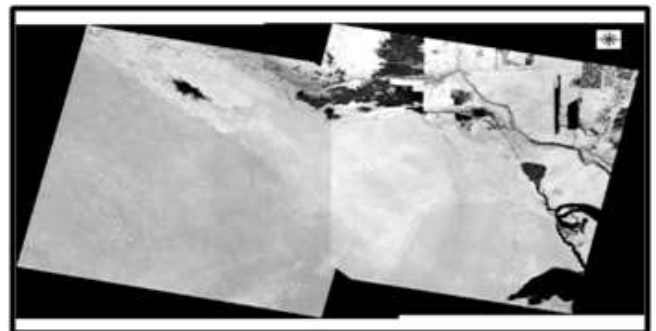


Figure 9: Mosaic Landsat OLI (16/6/2015 and 23/6/2015) band (10) for two satellite images (Path/Row 166/39) and (Path/ Row 167/39)

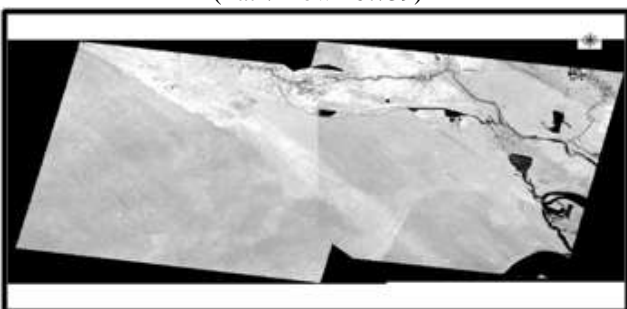


Figure 8: Mosaic Landsat ETM+ (6/6/2000 and 13/6/2000) band (6) for two satellite images (Path/Row 166/39) and (Path/ Row 167/39)

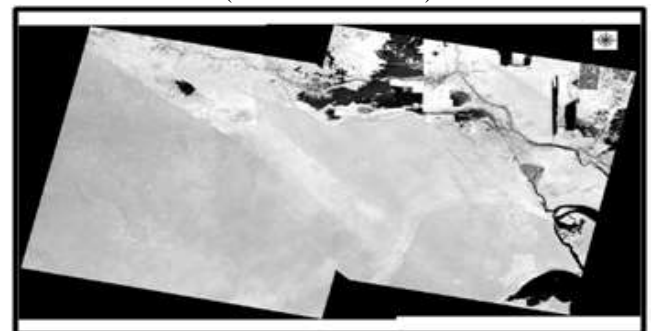


Figure 10: Mosaic Landsat OLI (5/6/2017 and 12/6/2017) band (10) for two satellite images (Path/Row 166/39) and (Path/ Row 167/39)

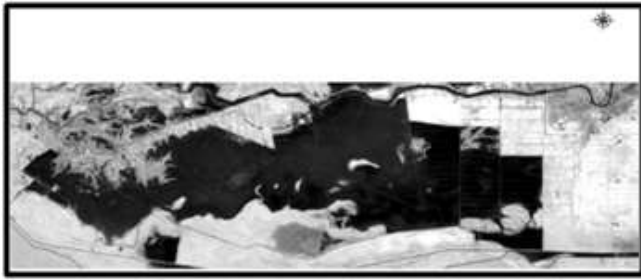


Figure 11: Landsat-5 (TM) Satellite Image (band 6). (1991), after applying Clipping process

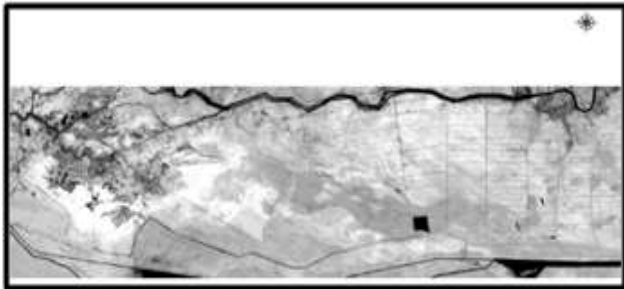


Figure 12: Landsat-7 (ETM+) Satellite Image (band 6), (2000) after applying Clipping process

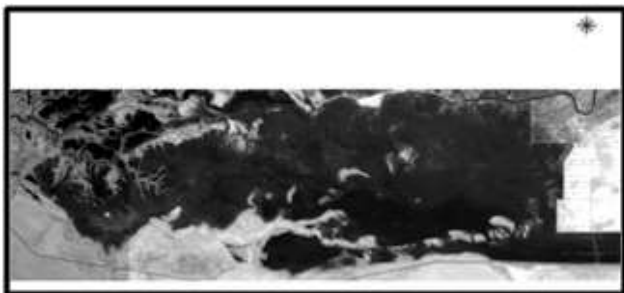


Figure 13: Landsat-8 (OLI) Satellite Image (band 10) (2015, after applying Clipping process.



Figure 14: Landsat-8 (OLI) Satellite Image (band 10) (2017), after applying Clipping process.

3.1 Conversion of thermal Digital number value to Temperature

The mono window algorithm is based on the premise that the brightness temperature at the satellite level can be retrieved from the thermal band data of Landsat, national Aeronautics and space Administration (NASA) has developed the equation (1) to compute the spectral radiance from DN value of Landsat data [7]. We import thermal band of satellite images for four years, which analysis depend to extract the surface temperature as follows:

1) Transfer the Digital Number (DN) to Spectral Radiance

The Landsat image storage at Digital Number (DN), DN value has no unit and physical connotation. The DN value range between 0 and 255, initially we performed Landsat (TM, ETM+ and OLI) calibration to convert DN to radiance/reflectance by using the following equation:

$$L_{\lambda} = \frac{(L_{\max} - L_{\min})}{(Q_{cal\max} - Q_{cal\min})} * (Q_{cal} - Q_{cal\min}) + L_{\min} \dots \dots \dots (1)$$

Where:

- L_{λ} : represents Spectral radiance at the sensor's aperture,
- L_{\min} and L_{\max} : represents the spectral radiances for each band at digital numbers 0 and 255, respectively.,
- Q_{cal} : represents the calibrated and quantized scaled radiance in unit of digital numbers=DN,
- $Q_{cal\min}$: represents the minimum quantized calibrated pixel value (corresponding to L_{\min}) in DN= 0,
- $Q_{cal\max}$: represents the maximum quantized calibrated pixel value (corresponding to L_{\max}) in DN= 255.

2) Conversion Spectral Radiance to surface Temperature

The spectral radiance was converted to surface temperature by using the following equation [8]:

$$T_{kelvin} = \frac{K_2}{\ln\left(\frac{K_1}{L_{\lambda}} + 1\right)} \dots \dots \dots (2)$$

Where: T represents the effective temperature in Kelvin, K_1 and K_2 represents calibration constants. The values of these constants can be shown in table 1 for the thermal band of TM ETM+ and OLI satellite image.

Table 1: Thermal bands calibration constant of TM ETM+ and OLI [9]

Constant	$K_1 (Wm^{-2}sr^{-1}\mu m^{-1})$	$K_2 (Kelvin)$
Landsat 5-TM	607.76	1260.56
Landsat 7-ETM+	666.09	1282.71
Landsat 8 OLI	774.89	1321.08

The spectral radiance can be converted to brightness temperature of thermal band in Celsius using the following formula: [10]

Finally, the output images are classified into different classes using level slicing technique for better understanding of the temperature variation of the marsh land. The thermal pattern distribution of the extracted surface temperature of Al-Hammar marsh for years 1991, 2000, 2015, and 2017 are shown in figures (15-18), respectively. Descriptive statistics including minimum, maximum, average and standard deviation of land surface temperature (LST) of Al-Hammar marshes for years 1991, 2000, 2015 and 2017 are presented in table (2-5), respectively

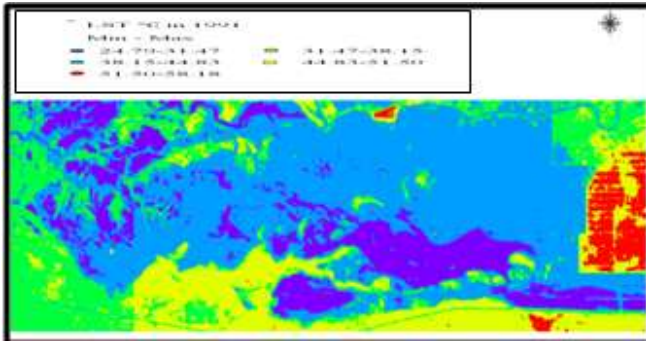


Figure 15: Thermal distribution map of Al-Hammar Marshes for year 1991

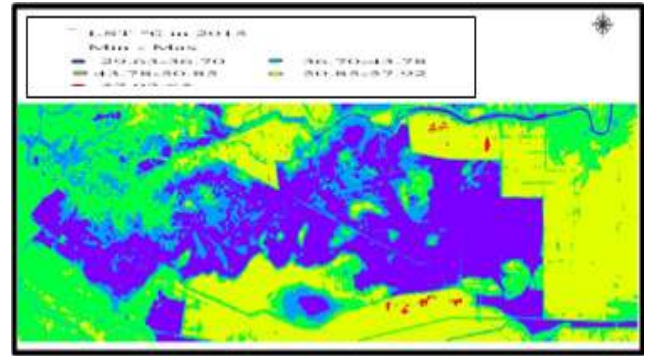


Figure 17: The thermal distribution map of Al-Hammar Marshes for year 2015

Table 2: Statistical significant of Al- Hammar marshes for year 1991

Class Color	Minimum temp. (°C)	Maximum Temp. (°C)	Average Temp. (°C)	Standard Deviations	Area Percentage
Blue	24.79	31.47	30.41	1.285	15.23%
Sky blue	31.47	38.15	33.51	1.576	46.38%
Green	38.15	44.83	42.11	1.908	19.53%
yellow	44.83	51.50	47.94	1.706	15.44%
Red	51.50	58.18	53.56	1.357	3.39%
	Total for all classes			7.832	99.97%
	Mean temp. (°C)		41.506		

Table 4: Statistical significant of Al- Hammar marshes for year 2015

lass Color	Minimum temp. (°C)	Maximum Temp. (°C)	Average Temp. (°C)	Standard Deviations	Area Percentage
Blue	29.63	36.70	33.16	1.53	27.74%
Sky blue	36.70	43.78	40.24	2.29	14.53%
Green	43.78	50.85	47.31	2.03	28.32%
yellow	50.85	57.92	54.38	1.65	29.17%
Red	57.92	65	61.46	0.64	0.21%
	Total for all class			8.14	99.97%
	Mean temp. (°C)		47.31		

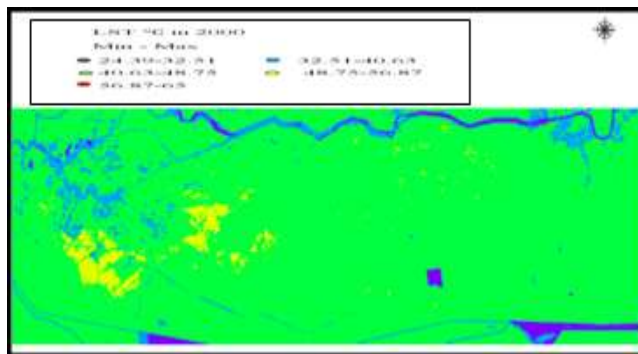


Figure 16: The thermal distribution map of Al-Hammar Marshes for year 2000

Table 3: Statistical significant of Al- Hammar marshes for year 2000

Class Color	Minimum temp. (°C)	Maximum Temp. (°C)	Average Temp. (°C)	Standard Deviations	Area Percentage
Blue	24.39	32.51	28.45	2.35	1.76%
Sky blue	32.51	40.63	36.57	2.05	4.64%
Green	40.63	48.75	44.69	1.71	85.91%
yellow	48.75	56.87	52.81	0.96	7.67%
Red	56.87	65	60.93	2.08	0.002%
	Total for all class			9.15	99.98%
	Mean temp. (°C)		44.69		

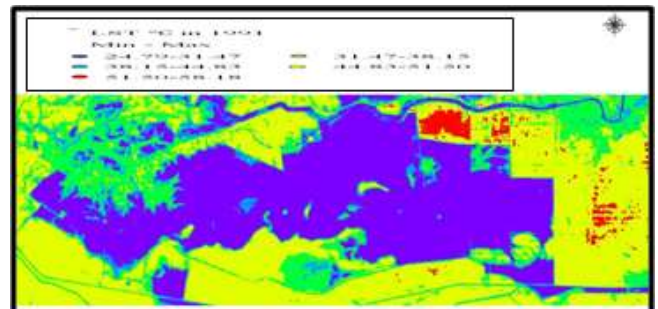


Figure 18: Thermal distribution map of Al-Hammar Marshes for year 2017

Table 5: Statistical significant of Al- Hammar marshes for year 2017

Class Color	Minimum temp. (°C)	Maximum Temp. (°C)	Average Temp. (°C)	Standard Deviations	Area Percentage
Blue	30.70	37.56	34.13	1.46	35.49%
Sky blue	37.56	44.42	40.99	2.13	7.12%
Green	44.42	51.28	47.85	1.9	17.47%
yellow	51.28	58.14	54.71	1.59	38.16%
Red	58.14	65	61.57	0.98	1.73%
	Total for all class			15.88	99.986%
	Mean temp. (°C)		47.85		

4. Conclusions

The temperature variation is derived from TM, ETM+, and OLI sensor thermal bands with the help of Landsat 7 science data users handbook and Landsat 8 data users handbook procedures. Thus the temperature is estimated for Al-Hammer marshes satellite images with different spectral resolution for years 1991, 2000, 2015, and 2017. The results indicated that the area percentage of blue (water) and

sky blue (shallow water) represent in year 1991 (61.61%) from the total area and the surface temperature is between (24.79-38.15°C) , in year 2000 was (6.4%) from the total area and surface temperature was between (24.39-40.63°C), in year 2015 was (42.27 %) from the total area and surface temperature was (29.63-43.78°C), in year 2017 was (42.61 %) from the total area and surface temperature was (30.70-44.42°C).. Also we found that some region have surface temperature more than 65°C due to intrusion of mining effect on the nearby area.

References

- [1] John R. Jensen (2009), "Remote Sensing of the Environment An Earth Resource Perspective", Second Edition, Dorling Kindersley, Delhi
- [2] Sun. D, Pinker. T (2004), "Case study of Soil Moisture effect on Land Surface Temperature Retrieval", IEEE Geoscience And Remote Sensing Letters. Vol.1. No.2:127-130.
- [3] F. Becker and Z.-L.Li, (1990). "Towards a local split window method over land surfaces," *International Journal of Remote Sensing*, vol.11, no. 3, pp. 369–393, .
- [4] MdShahid Latif 2014, "Land Surface Temperature Retrieval of Landsat-8 Data Using Split Window Algorithm- A Case Study of Ranchi District". *International Journal of Engineering Development and Research*
- [5] Sajad Zareie¹, Hassan Khosravi², Abouzar Nasiri³, and Mostafa Dastorani (2016) "Using Landsat Thematic Mapper (TM) sensor to detect change in land surface temperature in relation to land use change in Yazd, Iran", (*Solid Earth*, 7, 1551–1564,
- [6] Suresh. S¹, Ajay Suresh. V², Mani. K³, - (2016) "Estimation of Land Surface Temperature of High Range Mountain LandScape of Devikulam Taluk using Landsat 8 Data" *IJRET: International Journal of Research in Engineering and Technology*. Volume: 05 Issue: 01 | Jan
- [7] Markham, B.L., and Barker, J.L., (1996) "Landsat-MSS and TM post calibration dynamic ranges, atmospheric reflectance and at – satellite temperature", .p.3-8.
- [8] Schott, J.R., and Volchok, W.J., Yhematic (1985) "Mapper thermal infrared calibration. photogrametric Engineering and Remote ensin., 51:p.1351-1357,
- [9] "The Landsat 7 Science Data User's Handbook", (<http://www.usgs.gov/>)
- [10] "Landsat 8 (L8) Data User's Handbook", (<http://www.usgs.gov/>)